Available online at www.sciencedirect.com
ScienceDirect
Journal of Molecular Catalysis A: Chemical 265 (2007) 153–158
JOURNAL OF MOLECULAR CATALYSIS A: CHEMICAL
www.elsevier.com/locate/molcata

Semiconductor-catalyzed solar photooxidation of iodide ion

C. Karunakaran *, P. Anilkumar

Department of Chemistry, Annamalai University, Annamalainagar 608002, Tamilnadu, India

Received 19 May 2006; received in revised form 4 October 2006; accepted 11 October 2006
Available online 17 October 2006

Abstract

With natural sunlight TiO_2 (anatase), ZrO_2, MoO_3, Fe_2O_3, ZnO, CeO_2 and Al_2O_3 microparticles photocatalyze the oxidation of iodide ion but CuO, ZnS, CdO, CdS, HgO, PbO, Sb_2O_3 and Bi_2O_3 microparticles do not. The photocatalysis is not slowed down at least up to 120 min with ZrO_2, MoO_3, Fe_2O_3, CeO_2 and Al_2O_3 whereas it is 45 min with TiO_2 and 30 min with ZnO. The iodine generation depends on $[I^-]$, surface area and pH and is enhanced by the addition of ethanol. The catalysts show sustainable photocatalysis. Nanoparticles exhibit higher photocatalytic activities than microparticles. The catalytic efficiencies are of the order: $Fe_2O_3 > MoO_3 > TiO_2 > CeO_2 > ZnO > ZrO_2 > Al_2O_3$.

Keywords: Photocatalysis; Semiconductor; Sunlight; Iodide ion; TiO_2; ZrO_2; MoO_3; Fe_2O_3; ZnO; CeO_2; Al_2O_3

1. Introduction

Harnessing solar radiation is a means of sustainable, eco-friendly energy generation. Production of energy bearing chemicals through thermodynamically uphill reactions is the objective of solar energy conversion and storage and one such reaction is iodide ion oxidation ($\Delta G^\circ = +51.6\,kJ\,mol^{-1}$). Further, light-to-electrical energy conversion is possible through the oxidation of iodide ion at TiO_2 electrodes in photodriven electrochemical cells [1]. Although photocatalyzed oxidation of iodide ion on TiO_2 [2–6], colloidal TiO_2 [7], Pt-loaded TiO_2 [8], TiO_2 sensitized with phthalocyanines [9] and flower pigment cyanidin [10], ZrO_2, V_2O_5, Fe_2O_3, ZnO and Al_2O_3 [6] using artificial UV light have been made there is no report with natural sunlight and hence this work. The problem of fluctuation of sunlight intensity even under clear sky is overcome by carrying out set of experiments simultaneously, side-by-side, thus making the quantum of sunlight absorbed in the set of experiments identical.

2. Experimental

2.1. Materials

2.1.1. Microparticles

TiO_2 (Merck), ZrO_2 (Chemco, India), V_2O_5 (Johnson Matthey), MoO_3 (SD Fine, India), Fe_2O_3 (Fischer, India), CuO (SD Fine, India), ZnO (Merck), ZnS (SD Fine, India), CdO (Chemco, India), CdS (Chemco, India), HgO yellow (Chemco, India), HgO red (SD Fine, India), CeO_2 (SD Fine, India), Al_2O_3 (Merck), SnO_2 (BDH), PbO (Fischer, India), Pb_2O_3, PbO_2 (BDH), Sb_2O_3 (Qualigens, India), Bi_2O_3 (SD Fine, India), KI (Qualigens, India), KBr (SD Fine, India) and KCl (Merck) were used as received. Deionized distilled water was employed throughout the study. The TiO_2 used is of anatase form (99%+); the XRD pattern of the sample totally matches with the standard pattern of anatase (JCPDS) and the rutile lines are insignificant (Siemens D-5000 XRD, Cu Kα X-ray, $\lambda = 1.54$ Å, scan: 5–60°, scan speed: $0.2^\circ\,s^{-1}$). The BET surface areas were determined as: TiO_2 14.68, ZrO_2 15.12, V_2O_5 16.14, Fe_2O_3 17.84, CuO 1.51, ZnO 12.16, ZnS 7.67, CdO 14.45, CdS 15.47, HgO 6.39, CeO_2 11.0, Al_2O_3 10.63, SnO_2 114.7, PbO 0.28, PbO_2 1.95, Bi_2O_3 2.75 $m^2\,g^{-1}$; the corresponding values for MoO_3 and Pb_2O_3 are too small to be determined by BET method. The particle sizes, measured using particle sizer Horiba LA-910

* Corresponding author. Tel.: +91 4144221820.
E-mail address: karunakaranc@rediffmail.com (C. Karunakaran).

1381-1169/$ – see front matter © 2006 Elsevier B.V. All rights reserved.
doi:10.1016/j.molcata.2006.10.016

or Malvern 3600E (focal length 100 mm, beam length 2.0 mm, wet (methanol) presentation), are as below: TiO_2: 2.6–27.6, ZrO_2: 3.5–27.6, V_2O_5: 8.5–57.7, MoO_3: 4.19–19.3, Fe_2O_3: 2.6–27.6, CuO: 5.69–30.5, ZnO: 3.5–27.6, ZnS: 0.115–2.60, CdO: 2.6–11.4, CdS: 3.0–9.8, HgO (yellow): 0.17–5.69, CeO_2: 0.23–10.5, Al_2O_3: 2.6–57.7, SnO_2: 1.15–17.4, PbO: 4.47–13.3, Pb_2O_3: 0.20–7.72, PbO_2: 1.95–10.5, Bi_2O_3: 0.17–0.49 μm; the detailed distributions are given as supplementary materials.

2.1.2. Nanoparticles

TiO_2 P25 Degussa (ca. 80% anatase, 20% rutile) of mean particle size 30 nm and BET surface area ~50 $m^2\ g^{-1}$, TiO_2 anatase Hombikat (Fluka) of surface area ≥300 $m^2\ g^{-1}$, TiO_2 anatase nanopowder (99.7%, Sigma–Aldrich) of average particle size 15 nm and BET surface area 190–290 $m^2\ g^{-1}$, WO_3 nanoparticles (Sigma–Aldrich) of average diameter 49.6 nm and of surface area 16.9 $m^2\ g^{-1}$, ZnO nanoparticles (Sigma–Aldrich) of mean particle size 50–70 nm and of surface area 15–25 $m^2\ g^{-1}$ were used as supplied.

2.2. Method

The semiconductor-catalyzed solar photooxidations were carried out with AM 1 sunlight under clear sky in summer (March–July). The intensity of sunlight (W m^{-2}) was measured using Global pyranometer, MCPT, supplied by Industrial Meters, Bombay; the solar radiation was beyond the range of measurement of lux meter Lx-101A, Lutron, Taiwan, far larger than the upper limit of 50,000 lx. As near UV and visible light up to 560 nm is effective in photoexcitation of the active semiconductors employed in this study, the intensity of solar radiation (einstein $L^{-1}\ s^{-1}$) was also determined using ferrioxalate actinometer, which covers a wavelength range of 250–577 nm; under the experimental conditions, 440 W m^{-2} corresponds to 22 μeinstein $L^{-1}\ s^{-1}$. Fresh solutions of KI of required concentrations were taken in wide cylindrical glass vessels of uniform diameter and appropriate height; the catalyst powder covered the entire bottom of the vessel. 50 mL of the solution was air saturated and used for each experiment. The iodine formed was determined from the absorbance of the illuminated solution, measured at 350 nm using Hitachi U-2001 spectrometer; calibration curve was constructed for each KI concentration.

3. Results and discussion

3.1. Effective semiconductors

TiO_2 anatase (bandgap energy, E_g 3.2 eV [11]), ZrO_2 (E_g 5.0 eV [11]), MoO_3 (E_g 2.9 eV [12]), Fe_2O_3 (E_g 2.2 eV [11]), ZnO (E_g 3.2 eV [11]) and CeO_2 (E_g 3.4 eV [13]) catalyze the solar photooxidation of iodide ion whereas CuO (E_g 1.7 eV [11]), ZnS (E_g 3.6 eV [11]), CdO (E_g 2.2 eV [11]), CdS (E_g 2.4 eV [11]), HgO yellow (E_g 1.9 eV [11]), HgO red (E_g 1.9 eV [11]), PbO (E_g 2.8 eV [11]), Sb_2O_3 (E_g 3.0 eV [11]), and Bi_2O_3 (E_g 2.8 eV [11]) fail; V_2O_5 (E_g 2.8 eV [11]) dissolves, Pb_2O_3 oxidizes iodide ion in dark and PbO_2 (E_g 1.4 eV [14]) reacts with iodide. Although SnO_2 (E_g 3.5 eV [11]) photocatalyzes the oxidation (85 μM iodine liberated in 30 min from 50 mL of 0.05 M KI solution using AM 1 sunlight with a catalyst bed of 15.1 cm^2 and a catalyst loading of 2.0 g) it liberates iodine in dark as well (8 μM under identical conditions but in dark). The results with insulator Al_2O_3 (E_g 9.0 eV [13]) under identical conditions provide a comparison. Fig. 1, the UV–vis spectra of the air saturated KI solution illuminated with AM 1 sunlight and recorded at 10-min intervals, shows formation of iodine; the spectrum is similar to that of the authentic iodine–iodide solution. Chemical tests also confirm the formation of iodine; the solution turns purple with starch and discharged by thiosulfate.

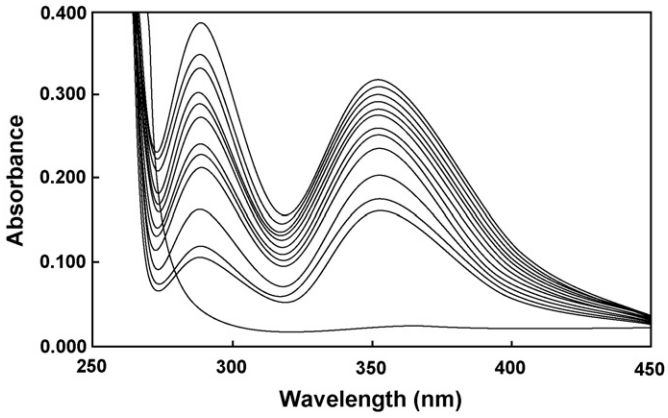

Fig. 1. Fe_2O_3-catalyzed solar photooxidation of I^-. The UV–vis spectra of AM 1 sunlight illuminated KI solution diluted five-times and recorded at 10 min intervals (↑); [I^-] = 0.05 M, Fe_2O_3 bed: 15.1 cm^2, Fe_2O_3 loading = 2 g, volume of air saturated KI solution = 50 mL.

3.2. Obtaining solar results

The measurement of solar radiation (W m^{-2}) shows fluctuation of sunlight intensity during the course of the experiment even under clear sky. Also, the sunlight intensity differs from day to day. Now, the sunlight intensity for a set of solar experiments of required reaction conditions was kept identical by carrying out the experiments simultaneously, side-by-side, thus making possible the comparison of the solar results.

The solar photogeneration of iodine from air saturated KI solution is not slowed down at least up to 120 min with Fe_2O_3, MoO_3, ZrO_2, CeO_2 and Al_2O_3 as catalysts while it is 45 minutes with TiO_2 and 30 min with ZnO as catalysts. Fig. 2 presents the formation of iodine from air saturated KI solution with TiO_2, ZrO_2, MoO_3, Fe_2O_3, ZnO, CeO_2 and Al_2O_3 as catalysts using AM 1 sunlight under identical sunlight intensities; the experiments were carried out simultaneously, side-by-side, under clear sky. The fluctuation of sunlight intensity during this study was insignificant. As the generation of iodine is uniform at least up to 30 min of illumination the iodine-formation rates were obtained by estimating iodine after 30 min irradiation in all the cases. The slowdown of the formation of iodine on prolonged illumination is not unknown; the UV photooxidation of iodide ion with platinum-loaded TiO_2 [8] and with TiO_2 but sensitized with phthalocyanines [9] show similar results. The results of TiO_2, ZrO_2, MoO_3, Fe_2O_3, ZnO, CeO_2 and Al_2O_3-catalyzed solar photooxidations are consistent. For each catalyst, a couple

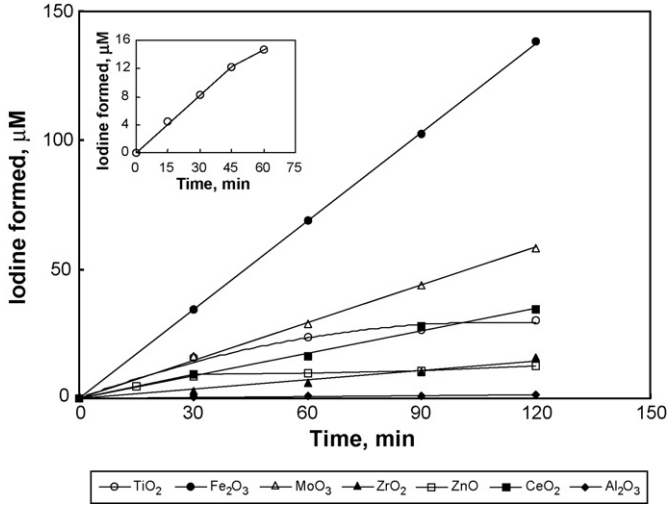

Fig. 2. Photooxidation of I^- on TiO_2, Fe_2O_3, MoO_3, ZrO_2, ZnO, CeO_2 and Al_2O_3 with AM 1 sunlight under identical intensities (Inset shows linearity up to 45 min). $[I^-] = 0.05$ M, catalyst bed = 15.1 cm^2, catalyst loading = 2.0 g, volume of air saturated KI solution = 50 mL.

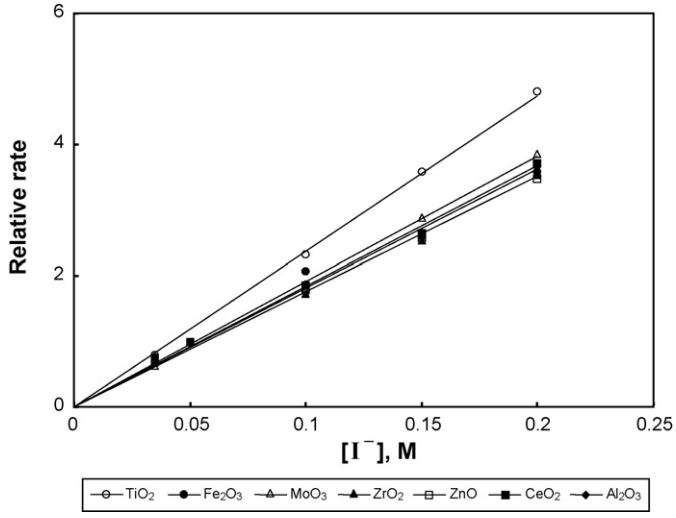

Fig. 3. Iodine formation as a function of $[I^-]$. Catalyst bed: 15.1 cm^2, catalyst loading = 2.0 g, volume of air saturated KI solution = 50 mL.

of solar experiments of identical reaction conditions carried out simultaneously, side-by-side, yield results with in ±6% and this is so on different days. This consistency is not surprising as the quantum of light absorbed per unit area is the same in control and text experiments. The photoactive metal oxides do not oxidize iodide ion in dark, confirmed by experiments under identical conditions but in dark.

3.3. Factors influencing photocatalysis

The influence of operational parameters such as $[I^-]$, area of the catalyst and pH on the photoformation of iodine in each catalysis was studied separately; the sunlight intensity in each study was kept identical by performing a set of experiments simultaneously, side-by-side. For example, the photogeneration of iodine at different iodide ion-concentrations for a particular catalysis was determined simultaneously, side-by-side. Under identical sunlight intensity, the iodine-formation increases linearly with $[I^-]$; plot of iodine-formation rate versus $[I^-]$ is linear and this is so in all the stated seven active catalysts (slope: 1.2×10^{-7}, 5.4×10^{-8}, 3.1×10^{-7}, 5.4×10^{-7}, 9.5×10^{-8}, 5.5×10^{-8}, 2.9×10^{-9} s^{-1} for TiO_2, ZrO_2, MoO_3, Fe_2O_3, ZnO, CeO_2, Al_2O_3, respectively; figures not given). As the photogeneration depends on sunlight intensity and the sunlight intensity is not identical in all the photocatalysis, as they were carried out on different days, comparison of the rates is incorrect. But, relative rates, rates relative to that at a specified condition, deduced by dividing the actual rates by that at a specified condition, all determined simultaneously, side-by-side, yield rates independent of sunlight intensity. These rates also vary linearly with $[I^-]$ (Fig. 3). Also, the photoformation of iodine is a linear function of the apparent surface area of the catalyst. And, this is in accordance with the Langmuir-Hinshelwood model [15]. Plot of iodine-formation rate versus surface area of the catalyst bed is linear for all the active catalysts studied (slope: 0.12, 0.14, 0.84, 0.85, 0.09, 0.22, 0.01 nM cm^{-2} s^{-1} for TiO_2, ZrO_2, MoO_3, Fe_2O_3, ZnO, CeO_2, Al_2O_3, respectively; figures not given) and Fig. 4 is the corresponding plot of relative rates. Fig. 5 presents the variation of iodine generation with pH; the pH was adjusted by the addition of HCl or NaOH and measured using a digital pH meter, after allowing the system to attain equilibrium. Except TiO_2 all the photocatalysts studied slow down the iodine-generation with increase of pH. TiO_2 enhances photoformation of iodine with increase of pH. Plots of actual rates provide similar profiles (slope: +1.4, −0.84, −0.86, −5.8, −0.77, −1.1, −0.16 nM s^{-1} for TiO_2, ZrO_2, MoO_3, Fe_2O_3, ZnO, CeO_2, Al_2O_3, respectively; figures not given). Measurement of pH before and after solar irradiation reveals a small drop in pH for all the photocatalysis examined. The metal oxides studied show sustainable photocatalytic activity; reuse of the photocatalysts yield identical results. Addition of ethanol enhances the photogeneration of iodine significantly in ZnO and ZrO_2 pho-

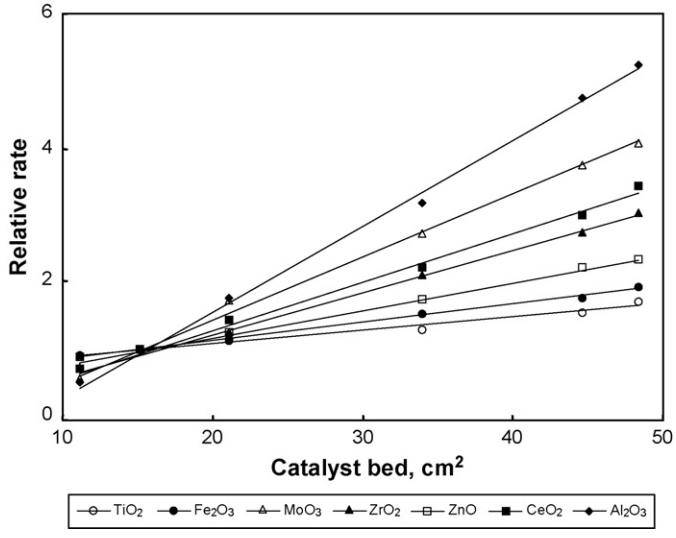

Fig. 4. Iodine formation as a function of area of catalyst bed. $[I^-] = 0.05$ M, catalyst loading = 2.0 g, volume of air saturated KI solution = 50 mL.

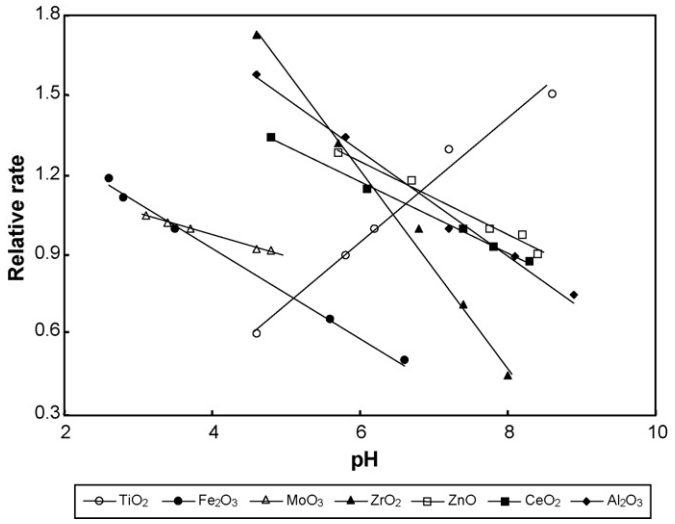

Fig. 5. Iodine formation as a function of pH. $[I^-] = 0.05$ M, catalyst bed = 15.1 cm^2, catalyst loading = 2.0 g, volume of air saturated KI solution = 50 mL.

tocatalysis, moderately in MoO_3 and TiO_2 catalysis and not so with CeO_2 and Al_2O_3 (Fig. 6).

3.4. Mechanism

Of the seven photocatalysts studied Al_2O_3 is an insulator providing a non-reactive surface while others are semiconductors with finite bandgap energies. Although ZrO_2 presents an absorption maximum around 250 nm, some samples show a non-negligible absorption in the near UV range (290–390 nm) and marginal photocatalysis occurs under irradiation in this range [16]. Illumination of the semiconductors with light of energy greater than the bandgap leads to bandgap excitation of semiconductors resulting in creation of electron–hole pairs; holes in the valence band and electrons in the conductance band. Since the recombination of photogenerated electron–hole pairs in semiconductors are so rapid, occurring in a picosecond time scale, for an effective photocatalysis the reactants are to be adsorbed on the photocatalysts [3]. The hole reacts with the adsorbed iodide ion to form an iodine atom that further reacts with iodide ion to produce I_2^-. The I_2^- disproportionates to form tri-iodide and iodide ions [3,7].

$$SC + h\nu \rightarrow h_{(vb)}^+ + e_{(cb)}^-$$

$$I_{(ads)}^- + h_{(vb)}^+ \rightarrow I$$

$$I + I^- \rightarrow I_2^-$$

$$2I_2^- \rightarrow I_3^- + I^-$$

In the presence of oxygen, transfer to the adsorbed oxygen molecule resulting in highly active superoxide radical-anion, $O_2^{\bullet -}$, effectively removes the electron [17].

$$O_{2(ads)} + e_{(cb)}^- \rightarrow O_2^{\bullet -}$$

$$O_2^{\bullet -} + e^- + 2H^+ \rightarrow H_2O_2$$

The H_2O_2 produced may oxidize iodide ion to iodine.

$$H_2O_2 + 2I^- \rightarrow I_2 + 2HO^-$$

Generally, adsorption of water on catalytic surfaces results in surface hydroxyl groups. Hole trapping by either the surface hydroxyl groups or adsorbed water molecules generates $^{\bullet}OH$ radicals, which are the primary oxidizing agents [17]. However, the clean first order dependence of iodine formation on $[I^-]$ discounts the possibility of $^{\bullet}OH$ radicals as the primary oxidizing species of I^-. If the photooxidation of I^- were primarily due to the $^{\bullet}OH$ radicals generated, the iodine formation should not linearly depend on $[I^-]$; the $^{\bullet}OH$ radicals are short lived and react almost instantaneously demanding non-dependence of the photooxidation rate on $[I^-]$. Also, this is in agreement with the study using terephthalic acid as a fluorescence probe for the quantitative measurement of $^{\bullet}OH$ production in TiO_2 photocatalysis; the oxidative reactions on TiO_2 occur mainly via photogenerated holes, not via $^{\bullet}OH$ [18].

$$^-OH_{(ads)} + h_{(vb)}^+ \rightarrow {}^{\bullet}OH$$

$$H_2O_{(ads)} + h_{(vb)}^+ \rightarrow {}^{\bullet}OH + H^+$$

Semiconductor-catalyzed photoreactions are generally governed by Langmuir–Hinshelwood kinetics [6,15] and the observed first order dependence on $[I^-]$ points to insignificant adsorption of iodide ion on the catalysts. The adsorption of anionic species on the metal oxides depends also on the surface excess charge on the semiconductor particles. At pH higher than the point of zero charge (PZC), the catalyst surface is negatively charged leading to electrostatic repulsion between iodide ion and the semiconductor particles. Hence, the concentration of iodide ion at the surface, in the double layer, is likely to be smaller than that in the bulk of the solution; the adsorption isotherm becomes linear leading to a first order kinetics of the photocatalysis. However, examination of Fig. 5 reveals,

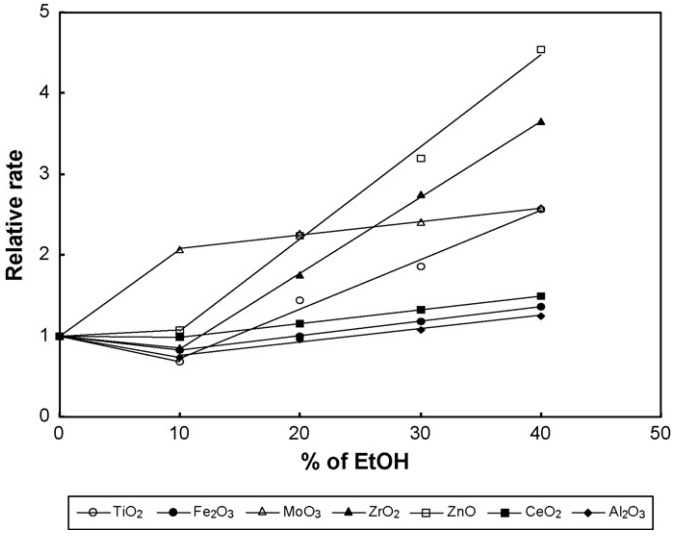

Fig. 6. Iodine formation as a function of ethanol content. $[I^-] = 0.05$ M, catalyst bed = 15.1 cm^2, catalyst loading = 2.0 g, volume of air saturated KI solution = 50 mL.

for some catalysts at least (TiO_2 and ZrO_2), uniform trend in the photocatalysis at pH higher as well as lower than PZC; the PZC for TiO_2, ZrO_2, Fe_2O_3 and ZnO are 5.80, 6.70, 8.60 and 8.80, respectively [11]. A possible explanation is the modification of PZC values in presence of ions in solution [19,20]; the PZC for TiO_2 lowers from 6.4 to 4.5 [19]. Hence it is possible that the PZC values for the photocatalysts in presence of ions are lower than the experimental pH. Significant enhancement of iodine-formation on the addition of ethanol, in some semiconductors at least, indicates hole trapping by alcohol and the generated radicals oxidize iodide ions.

Non-reactive surfaces such as Al_2O_3 provide an ordered two-dimensional environment for effective electron transfer from the donor to the acceptor. Either the donor iodide ion or the acceptor oxygen molecule, both adsorbed on the photocatalyst, may undergo photoexcitation followed by electron transfer. The donor excitation results in the transfer of excited electron whereas the acceptor excitation leads to an electron jump from the donor level to the vacant acceptor level [3]. The lack of enhancement of iodine-generation by ethanol in Al_2O_3-photocatalysis is on expected lines; due to the absence of generation of holes on Al_2O_3 there could be no hole trapping by adsorbed alcohol.

3.5. Comparison of photocatalytic efficiencies

Comparison of the photocatalytic efficiencies reveal the order: Fe_2O_3 (4.5) > MoO_3 (1.5) > TiO_2 (1.0) > CeO_2 (0.90) > ZnO (0.82) > ZrO_2 (0.38) > Al_2O_3 (0.08); the solar photooxidations were carried out under identical AM 1 sunlight intensity and reaction conditions (0.05 M KI, catalyst bed: 15.1 cm^2, catalyst loading = 2.0 g, volume of KI solution = 50 mL, illumination = 30 min); the relative efficiencies are given in parentheses. The observed photocatalytic efficiencies are in line with the bandgap energies. The highly active Fe_2O_3 (optical absorption edge 620 nm [21]) can be photoexcited with visible light whereas the least active semiconductor ZrO_2 requires UV light for photoactivation. The bandgap energies of TiO_2, ZnO and CeO_2 are very close (optical absorption edges 380, 396, 440 nm, respectively [21]) and hence the catalytic efficiencies. MoO_3 (optical absorption edge 443 nm [21]) shows a better catalytic activity as it is susceptible to photoexcitation with visible light.

3.6. Photocatalysis by nanoparticles

Semiconductor nanoparticles are effective photocatalysts. Experiments with nanoparticles and microparticles, under AM 1 sunlight of identical intensity and under identical conditions (0.05 M KI, catalyst bed: 11.1 cm^2, catalyst loading = 0.02 g, volume of KI solution = 25 mL, illumination = 30 min), reveal the higher photocatalytic efficiencies of nanoparticles compared to the microparticles. Also, purging of air (7.8 mL s^{-1}) marginally improves the efficiency of photocatalysis by TiO_2 Hombikat and TiO_2 P25 Degussa. The photocatalytic efficiencies are of the order: TiO_2 nanopowder, Sigma–Aldrich (6.1, 6.6) > TiO_2 Hombikat, Fluka (3.6, 5.5) > TiO_2 P25 Degussa (3.0, 4.2) > TiO_2 anatase microparticles, Merck (1.0, 1.1); the relative efficiencies with air saturated and continuous air purging are given in parentheses. Unlike TiO_2, ZnO and WO_3 nanopowders do not form suspension but settle at the bottom even on continuous air purging. As the catalyst loading is very small, they do not cover the entire bottom of the reaction vessel and hence there is no effective catalyst bed.

3.7. Lack of photooxidation of chloride and bromide ions

Experiments under identical conditions with all the microparticles and the nanoparticles stated show absence of photooxidation of chloride and bromide ions. Irradiation of air saturated 0.2 M KCl or KBr solutions (25 mL) over the microparticles (catalyst bed = 15.1 cm^2, catalyst loading = 1.0 g) with natural sunlight for 5 h fails to show positive results; only ZnO feebly photooxidizes chloride ion in traces. Similar experiments with TiO_2 nano- and micro-particles (0.02 g) under suspension in air saturated 0.2 M KCl or KBr solutions with an illumination area of 15.1 cm^2 do not show oxidation of chloride or bromide ions even on irradiation with sunlight for 5 h.

4. Conclusions

TiO_2 (anatase), ZrO_2, MoO_3, Fe_2O_3, ZnO, CeO_2 and Al_2O_3 microparticles photocatalyze the oxidation of iodide ion with natural sunlight and the influence of $[I^-]$ and also surface area on the generation of iodine is similar with all the photocatalysts reported. While the increase of pH favors TiO_2-photocatalysis it is the other way with other catalysts. The catalytic efficiencies are in line with the bandgap energies. Nanoparticles show better photocatalytic efficiencies than microparticles.

Acknowledgements

The authors thank the University Grants Commission, New Delhi, for the financial support through major research grant no F.12-64/2003 (SR) and *Degussa* for gifting TiO_2 P25 sample. PA is grateful to UGC for PF.

Appendix A. Supplementary data

Supplementary data associated with this article can be found, in the online version, at doi:10.1016/j.molcata.2006.10.016.

References

[1] B. O'Regan, N. Gratzel, Nature 353 (1991) 737.
[2] K. Ishibashi, A. Fujishima, T. Watanabe, K. Hashimoto, J. Photochem. Photobiol. A 134 (2000) 139.
[3] A.L. Linsebigler, G. Lu, J.T. Yates Jr., Chem. Rev. 95 (1995) 735.
[4] P.V. Kamat, Chem. Rev. 93 (1993) 267.
[5] G.P. Lepore, C.H. Langford, J. Vichova, A. Vicek Jr., J. Photochem. Photobiol. A 75 (1993) 67.
[6] C. Karunakaran, S. Senthilvelan, S. Karuthapandian, K. Balaraman, Catal. Commum. 5 (2004) 283.
[7] D.J. Fitzmaurice, M. Eschle, H. Frei, J. Phys. Chem. 97 (1993) 3806.
[8] T. Ohno, K. Fujihara, S. Saito, M. Matsumura, Sol. Energy Mater. Sol. Cells 45 (1997) 169.

[9] J. Hodak, C. Quinteros, M.I. Litter, E.S. Roman, J. Chem. Soc., Faraday Trans. 92 (1996) 5081.
[10] K. Tennakone, A.R. Kumarasinghe, G.R.R.A. Kumara, K.G.U. Wijayantha, P.M. Sirimanne, J. Photochem. Photobiol. A 108 (1997) 193.
[11] Y. Xu, M.A.A. Schoonen, Am. Mineral. 85 (2000) 543.
[12] Y. Zhao, J. Liu, Y. Zhou, Z. Zhang, Y. Xu, H. Naramoto, S. Yamamoto, J. Phys.: Condens. Matter 15 (2003) L547.
[13] C. Sol, R.J.D. Tilley, J. Mater. Chem. 11 (2001) 815.
[14] A. Kumar, A. Henglein, H. Weller, J. Phys. Chem. 93 (1989) 2262.
[15] C. Karunakaran, S. Senthilvelan, J. Mol. Catal. A 233 (2005) 1.
[16] S.G. Botta, J.A. Navio, M.C. Hidalgo, G.M. Restrepo, M.I. Litter, J. Photochem. Photobiol. A 129 (1999) 89, and the references cited therein.
[17] D. Chatterjee, S. Dasgupta, J. Photochem. Photobiol. C 6 (2005) 186.
[18] K-i. Ishibashi, A. Fujishima, T. Watanabe, K. Hashimoto, J. Photochem. Photobiol. A 134 (2000) 139.
[19] J. Gimenez, M.A. Aguado, S. Cervera-March, J. Mol. Catal. A 105 (1996) 67.
[20] J. Domenech, J. Munoz, Electrochim. Acta 32 (1987) 1383.
[21] M. Miyauchi, A. Nakajima, T. Watanabe, K. Nashimoto, Chem. Mater. 14 (2002) 2812.